

Accepted Manuscript

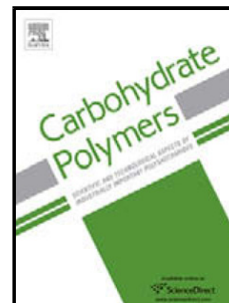
Title: Cell culture and characterization of cross-linked Poly(vinyl alcohol)-g-starch 3D scaffold for tissue engineering

Author: Wen-Chuan Hsieh Jiun-Jia Liao

PII: S0144-8617(13)00616-4

DOI: <http://dx.doi.org/doi:10.1016/j.carbpol.2013.06.020>

Reference: CARP 7838



To appear in:

Received date: 15-3-2013

Revised date: 10-6-2013

Accepted date: 13-6-2013

Please cite this article as: Hsieh, W.-C., & Liao, J.-J., Cell culture and characterization of cross-linked Poly(vinyl alcohol)-g-starch 3D scaffold for tissue engineering, *Carbohydrate Polymers* (2013), <http://dx.doi.org/10.1016/j.carbpol.2013.06.020>

This is a PDF file of an unedited manuscript that has been accepted for publication. As a service to our customers we are providing this early version of the manuscript. The manuscript will undergo copyediting, typesetting, and review of the resulting proof before it is published in its final form. Please note that during the production process errors may be discovered which could affect the content, and all legal disclaimers that apply to the journal pertain.

1 Cell culture and characterization of cross-linked Poly(vinyl
2 alcohol)-g-starch 3D scaffold for tissue engineering

3 Wen-Chuan Hsieh*, Jiun-Jia Liao

4
5 Department of Biological Science and Technology, I-Shou University, Kaohsiung 82445,
6 Taiwan R.O.C.

7
8 *Corresponding author. Tel: +886 7 6151100 ; fax: +886 7 6151959

9 E-mail: wenchuan@isu.edu.tw

10 **Highlights**

11 ► PVA and starch can be chemically cross-linked to form a PVA-g-starch 3D
12 scaffold-grafted polymer. ►The absorbency of PVA-g-starch 3D scaffold is up to 800%.
13 ► the strength of the 3D scaffold strength reaches 4×10^{-2} MPa. ►The 3D scaffold was
14 degraded by various enzymes at a rate of up to approximately 30-60% in 28 days. ► *In*
15 *vitro* experiments revealed that cells proliferate and grow in the 3D scaffold material.

16 **Abstract**

17 The research goal of this experiment is chemically to cross-link poly(vinyl alcohol)
18 (PVA) and starch to form a 3D scaffold that is effective water absorbent, has a stable
19 structure, and supports cell growth. PVA and starch can be chemically cross-linked to
20 form a PVA-g-starch 3D scaffold polymer, as observed by Fourier transform infrared
21 spectroscopy (FTIR), with an absorbency of up to 800%. Tensile testing reveals that, as
22 the amount of starch increases, the strength of the 3D scaffold strength reaches 4×10^{-2}
23 MPa. Scanning electron microscope (SEM) observations of the material reveal that the
24 3D scaffold is highly porous formed using a homogenizer at 500 rpm. In an enzymatic
25 degradation, the 3D scaffold was degraded by various enzymes at a rate of up to
26 approximately 30-60% in 28 days. *In vitro* tests revealed that cells proliferate and grow in

27 the 3D scaffold material. Energy dispersive spectrometer (EDS) analysis further verified
28 that the bio-compatibility of this scaffold.

29 **Keywords:** Cross-linking, PVA-g-starch, 3D scaffold, Biodegradation, Cell culture

30 **1. Introduction**

31 Biodegradable polymers have been extensively utilized in medicine for a long time.
32 Biodegradable polymer are bio-compatible, bio-absorbent and do not induce an immune
33 reaction or inflammation can be used in medical materials in, for example, sutures, cover
34 coatings, fracture fixing materials and other applications. (Wang, Wu, & Chen, 2004;
35 Jiang et al., 2004; Li et al., 2005, Hsieh et al., 2011; Kuo et al., 2012). In recent years, the
36 use of biodegradable polymer in combination with the cultivation of live cells to form
37 new cartilage tissue has opened up the new research field of tissue engineering (Lanza,
38 Langer, & Vacanti, 1999; Chen, Ushida, & Tateshi, 2000; Lahiji et al., 2000; Yoshimoto
39 et al., 2003). The aim of using these special biopolymers to construct 3D scaffolds in
40 which implanted cells can proliferate and grow, is to combine the advantages of the
41 transplantation of human tissue with those of synthetic repair materials, and so establish
42 principles for tissue engineering. Therefore, the use of biodegradable polymers in
43 applications of biomaterials seems more important than ever.

44 A 3D scaffold can be used to grow and cultivate cells only under the following
45 conditions, 1. Biocompatible scaffold must be non-toxic to implanted cells or tissues and
46 to promote their growth and adhesion. 2. Bio-absorbable or bio-decomposable a 3D
47 scaffold is an auxiliary tool, whose ultimate purpose is to be able to degradation and then
48 be absorbed or excreted by the body after the cells or tissues have grown in a period
49 suitable for cultivation. 3. Exhibit highly linked pores - when cells are being cultivated
50 using a 3D scaffold, they must be able to adopt the designed shape in the scaffold. As the
51 cells grow in the culture liquid, nutrients must be freely input to, and the waste material

52 should be excreted from, the structure. Accordingly, porosity is a key factor in cell
53 cultivation. 4. Exhibit excellent mechanical strength and flexibility - the cells will not be
54 unable to maintain their original shapes during the period of cultivation because of
55 changes in the culture liquid or degradation. Hence, 3D scaffold must have a mechanical
56 strength to support the attachment of cells.

57 This investigation concerns an inexpensive polymer-polyvinyl alcohol (PVA) which
58 is an extensively used water-soluble polymer. PVA contains numerous polar alcohol
59 groups and may form hydrogen bonds with water. It therefore dissolves easily in water.
60 PVA is also a biodegradable material that has been used in tissue engineering, and
61 production methods include electrospinning to form PVA nanofibrous scaffolds (Asran,
62 Henning, & Michler, 2010; Liao et al., 2011); chemical synthesis (Mansur & Costa, 2008;
63 Lynda et al., 2009), freeze-drying (Mohan & Nair, 2008; Mohan, Nair, & Tabata, 2010;
64 Poursamar, Azami, & Mozafari, 2011; Jiang, Liu, & Feng, 2011), and melt-molding
65 particulate-leaching (Oh et al., 2003). Starch, a natural polymer, is a material that is also
66 commonly used in tissue engineering. In most relevant studies starch is blended with
67 other matter to form a porous scaffold (Gomes et al., 2002; Ghosh et al., 2008; Santos et
68 al., 2010; Duarte, Mano, & Reis, 2010; Castillejo et al., 2012). Other methods of
69 producing a porous scaffold, such as chemical synthesis (Xiao & Yang, 2006; Sundaram,
70 Durance, & Wang, 2008), wet spinning (Pashkuleva et al., 2010; Rodringues et al., 2012),
71 and use of a blowing agent (Salgado et al., 2002) have also been reported upon in these
72 literature. The cross-linking method that is proposed in this investigation does not seem
73 to have been described before is utilized herein for the first time.

74 The goal is to exploit an existing, inexpensive, biodegradable material to form a 3D
75 scaffold material for use in regenerative medicine. Since PVA is inexpensive, easy to
76 obtain, highly biodegradable and biocompatibility, PVA and natural polymer-starch are
77 considered herein. No complex or expensive equipment is required: simple chemical
78 cross-linking method, to form 3D scaffold material and to improve its mechanical

79 properties and formation. Not only are the structural changes of the material examined:
80 its gel and swelling, formation, mechanical properties, biodegradability, porosity and
81 other characteristics are elucidated. Finally, NIH3T3 cells are transplanted and cultivated
82 to 3D scaffold, and observe the effectiveness of the material for tissue engineering.

83 **2. Experiment**

84 **2.1. Formation of 3D scaffold**

85 Poly(vinyl alcohol) (PVA) and soluble starch were obtained from the Nitto Chemical
86 Pharmaceutical Companies. Formaldehyde was obtained from Aldrich Chemical
87 Company. Sulfuric acid (H_2SO_4) was purchased from The First Chemical Company. All
88 materials and chemicals were used as acquired without any processing.

89 The starch powder (0.5, 0.75, & 1 g) was separately dissolved in RO water (10 mL)
90 at room temperature. The 1 g of PVA was dissolved in RO water (10 mL) at 90 °C. The
91 starch solution was slowly added into the PVA solution and mixed uniformly by a
92 homogenizer at 500 rpm with heating to 90 °C for 30 minutes, until the mixture was
93 viscous. The sample was then cooled to room temperature, before H_2SO_4 (3 mL) and
94 formaldehyde (1.25 mL) were added with stirring. Finally, the sample was poured into
95 the tube and placed in the oven at 60 °C for 50 minutes to form a circle shape.

96 **2.2. SEM analysis**

97 The morphology of 3D scaffold was observed under a field emission scanning
98 electron microscope (FE-SEM Hitachi-4700, Japan). The completely dried blank sample
99 was placed on a copper base, to which it was fastened with conductive tape. It was then
100 plated with platinum in a vacuum deposition machine, before being placed on the sample
101 base of FE-SEM for observation under the desired conditions of an accelerating voltage
102 of 10 kV at a working distance (WD) of 15 mm. Photographs of the enzyme-degraded
103 samples were also taken after the treatment processes. 3D scaffold sample with the

104 cultured cells was put in paraformaldehyde solution to dehydrate for 12 hours. It was then
105 freeze-dried. The substances on the surface of the sample were then analyzed by EDS
106 (HORIBA, Japan).

107 **2.3. FT-IR analysis**

108 The structure of the graft scaffolds were analyzed with FT-IR (Perkin Elmer FT-IR
109 Spectrum one, USA). The material with the cross-linked PVA-g-starch 3D scaffold was
110 placed in an oven to dehydrate. It was then placed in an FT-IR device for analysis.
111 Scanning was carried out and the spectrum at 400 cm^{-1} - 4000 cm^{-1} was recorded to
112 identify the changes in the functional groups in the PVA-g-starch 3D scaffold that were
113 caused by the above process.

114 **2.4. Swelling of PVA-g-starch scaffold**

115 The cross-linked PVA-g-starch 3D scaffold was dried in an oven at 50°C . The dried
116 PVA-g-starch 3D scaffold was immersed in distilled water at room temperature for 48
117 hours. Excess water was wiped from the swelled PVA-g-starch 3D scaffold and the
118 swelling ratio was calculated using the following below formula.

$$119 \quad \text{Swelling (\%)} = [(G_s - G_i) / G_i] \times 100$$

120 G_i represents the initial weight of the freeze-dried PVA-g-starch 3D scaffold, and G_s is
121 the weight of the colloid in the swelling state.

122 **2.5. Porosity**

123 The porosity of the PVA-g-starch 3D scaffold is calculated using the liquid
124 displacement method (Nie et al., 2012). The scaffold is submerged in water (V_1) exactly
125 for 30 minutes to ensure that enough liquid enters the pores of the scaffold. The new total
126 volume of the liquid and the liquid impregnated scaffold is V_2 . When the liquid
127 impregnated scaffold is removed, the remaining liquid volume is V_3 and the porosity is

128 given by,

$$129 \quad P (\%) = [(V1-V3) / (V2-V3)] \times 100$$

130 **2.6. Tensile test**

131 The mechanical properties of PVA-g-starch 3D scaffolds were examined by tensile
132 test (Shimadzu EZ tensile, Japan). The sample was placed in the tensile strength tester
133 under a load of 500 N. The tensile strength test was conducted at a rate of 5 mm/min, and
134 the variations in strain and stress of the scaffold were investigated as the maximum
135 breaking strength was approached.

136 **2.7. Biodegradability**

137 The biodegradability test was carried out to observe the degradation of PVA-g-starch
138 3D scaffold with over time. To simulate the environment of a human body, three enzymes
139 were used in this investigation. They were lipase (20 µg/ml), α-amylase (150.5 U) and
140 lysozyme (20 µg/ml). A thickness of approximately 0.5 cm of each processed 3D scaffold
141 was placed in a 15 mL centrifuge tube with 1mL buffer solution that could be used with
142 the various enzymes. Different concentrations of an enzyme were added. The centrifuge
143 tube was placed in a 37 °C 100 rpm vibrating thermostatic bath for 28 days to perform an
144 *in vitro* test. Every seven days, the 3D scaffold and placed in an environment at 25 °C to
145 dry in completely. The weight lost by the sample was measured each time. The
146 biodegradability is given by the following formula.

$$147 \quad \text{Biodegradability (\%)} = (W_0 - W_t) / W_0 \times 100\%$$

148 W_0 and W_t are the scaffold weights before and after the degradation.

149 **2.8. *In vitro* test**

150 Fibroblasts (NIH3T3 fibroblasts) were cultured in a petri dish with a diameter of 10
151 cm. The culture liquid comprised DMEM (Dulbecco's Modified Eagle's Medium), 10%

152 fortified bovine calf serum (FBS) and 1% penicillin streptomycin solution. Its pH value
153 was maintained at 7.4. The incubator settings were 37 °C with 5% CO₂ and 95% relative
154 humidity. The cell culture of PVA-g-starch scaffold which cycles lasted for three days.
155 The numbers of cells were counted every 24 hours. The data thus obtained were used to
156 plot the growth curve.

157 The cells that well detached from the trypsin were placed in a 15 mL centrifuge; the
158 medium was added in an amount equal to that of trypsin. The system was mixed by
159 centrifugation at 300 rcf and 4 °C for five minutes. Then, the supernatant was removed
160 and 2 mL of medium was subsequently added to form the cell solution. Approximately 1
161 × 1 × 0.1 cm of scaffold was placed in each of 24-wells plate, and 500 λ cell solutions
162 was added to the surface of the 3D scaffold in each 24-wells plate. The sample was
163 placed in an incubator with 5% CO₂ at 95% relative humidity and 37 °C for 30 minutes.
164 The scaffold was then removed from the incubator, and placed into another well with no
165 additional agents; 2 mL medium was added to initiate the cell attachment experiment.
166 After three days of culturing, the scaffold that contained the cells was immersed in 5 mL
167 10% formaldehyde overnight so that the cell was fixed to the scaffold, to prepare the test
168 sample for EDS analysis.

169 **3. Results and Discussion**

170 **3.1. Morphology of 3D scaffold**

171 SEM was utilized to observe the morphological changes of the chemical
172 cross-linked PVA-g-starch 3D scaffold. Fig. 1 presents SEM image of the PVA-g-starch
173 3D scaffold. The pores of the 3D material were formed by a homogenizer at 300 rpm.
174 The photographs display the distribution of the pores of the 3D material that was
175 cross-linked by stirring within the material. The physical properties of these materials
176 will be investigated, and the material will be used for cell cultivation.

177 3.2. FT-IR analysis of cross-linked PVA-g-starch

178 To confirm whether cross-linking had occurred in the PVA-g-starch 3D scaffold,
179 FT-IR was utilized to examine its structure. Fig. 2 displays the FT-IR spectra of PVA,
180 starch and the cross-linked PVA-g-starch 3D scaffold. Absorption peaks associated with
181 the methylene group (CH_2) of PVA are observed close to 3000 cm^{-1} , 1000 cm^{-1} , and 800
182 cm^{-1} ; a peak associated with the $\text{C}=\text{O}$ group are observed near 1700 cm^{-1} , and peaks
183 associated with the OH group are observed close to 1150 cm^{-1} and $3400\text{-}3640\text{ cm}^{-1}$. The
184 FT-IR absorption peak of functional group of PVA is also observed in the spectrum of the
185 cross-linked PVA-g-starch material. The CH_2 group of starch and the cross-linked 3D
186 scaffold appeared to yield a weaker FT-IR peak near 3000 cm^{-1} than did the CH_2 group of
187 PVA. Furthermore, the peak of the OH group in PVA close 1150 cm^{-1} gradually became
188 weaker upon cross-linking. Similar result has been reported by Lee and Xiao (Lee, Kung,
189 & Lee, 2005; Xiao & Yang, 2006), the cross-linking agent of Formaldehyde (aldehyde
190 group) can react with PVA and starch (hydroxyl groups) under the presence of an acid
191 catalyst, and forming rings structure of 1, 3-dioxane. The FT-IR absorption peaks of the
192 cross-linked PVA-g-starch demonstrate, significant changes in the major absorption peaks
193 upon cross-linking, implying that the PVA-g-starch had been successfully prepared.

194 3.3. Swelling ratio of 3D scaffold

195 A swelling ratio test was performed to determine the extent of swelling of the
196 PVA-g-starch 3D scaffold. It is very important high water content that support tissue
197 engineering, such as tissue-like elasticity, good exchange of nutrients for growth of cells.
198 Fig. 3 displays the rates of absorption of water by the PVA-g-starch 3D scaffold after the
199 cross-linking of PVA using various starch concentrations. The above histogram is the
200 actual forming photographs of the PVA-g-starch 3D scaffold. Fig. 3 demonstrates that,
201 the rate of water absorption increases significantly with the starch concentration. At a
202 PVA to starch concentration ratio of 1:0.5 (ST1), the swelling ratio was 400%; as the

203 starch concentration increased, the absorption of water considerably, yielding a swelling
204 ratio of 800%. Because of cross-linking with hydrophilic PVA and starch, forming 1,
205 3-dioxane rings structure, keep a number of water in the scaffold that causes
206 PVA-g-starch have a high swelling. However, absorption of water at ST2 (1:0.75) did not
207 differ much from that at ST3 (1:1), suggesting that PVA-g-starch 3D scaffold that was
208 cross-linked in ST2 (1:0.75) and ST3 (1:1) may have reached saturation level, reducing
209 the degree of water absorption.

210 **3.4. Tensile test**

211 The most important characteristic of a 3D scaffold that is to be used in tissue
212 engineering is that it has a particular strength, which enables it to support the cell while
213 maintaining its shape. The scaffolds with different mechanical properties should be
214 depending on the desired tissue engineering application. PVA and starch have much poor
215 mechanical properties. The addition of starch into PVA could reduce its solubility and
216 increase strength. Table 1 presents the mechanical properties of the cross-linked
217 PVA-g-starch 3D scaffold under wet state. Table 1 indicates that, as the starch
218 concentration increases, the tensile strength falls from 4.3×10^{-2} MPa for the ST1 sample
219 to 3.6×10^{-2} MPa for the ST3 sample, perhaps because more highly cross-linked starch
220 has a lower elasticity. However, regardless of concentration, the elongation ratio at
221 breakage of all cross-linked samples reaches 300%, indicating that the material is an
222 excellent elastomer. The young's modulus of the material is approximately $1.5-2.9 \times 10^{-2}$
223 GPa. In the porosity test, the porosities obtained when three starch concentration in the
224 formation of the 3D scaffold were all above 75%, above this value did not seem to
225 influence the strength of the 3D scaffold. PVA and starch are a hydrophilic polymer, and
226 not suitable for using as cell culture. Therefore, PVA need cross-linking another substance
227 to decrease solubility and giving strength for cell culture. These results demonstrate that
228 the cross-linked PVA-g-starch 3D scaffold had strength and porosity for transplanting

229 cells and the material will be used for cell cultivation in this study.

230 **3.5. Biodegradability of 3D scaffold**

231 As well as maintaining a minimum the required strength during cell culture, tissue
232 engineering implant materials must support the growth of cells, and the scaffold material
233 can slowly degrade into small molecules and excrete. Hence, to simulate the environment
234 of the human body, the enzymes lipase, α -amylase, and lysozyme are utilized in the
235 evaluation of the biodegradability of the scaffold. These three enzymes are all hydrolases.
236 Lipase is a lipid-digesting enzyme, which mainly affects which carbonyl group of
237 material. The α -amylase and lysozyme enzyme are carbohydrate-digesting enzymes, but
238 α -amylase degrades the α -1,4 bonds and lysozyme degrades the glycosidic bonds of β -1,4
239 bonds.

240 Fig. 4 plots the biodegradability of 3D scaffold in various enzymes. The extents of
241 enzymatic degradation rates with a PVA to starch ratio of 1:0.5 (ST1) after 28 days are
242 lipase 56%, α -amylase 46% and lysozyme 43%. However, the extent of enzyme
243 degradation falls as the starch concentration increases; the degree of cross-linking
244 therefore increases. With a PVA to starch ratio of 1:1 (ST3), after 28 days, the extents of
245 enzymatic degradation are lipase 27%, α -amylase 35% and lysozyme 31%. The high
246 concentration of starch is presumed to make the structure of scaffold denser and more
247 complete, making it more difficult for the enzymes to degrade. In the control group, the
248 material was placed in aqueous PBS water without enzymes. Although the weight loss
249 increased with the reaction time, the weight loss was insignificant, perhaps because
250 immersing the material in water and caused it to swell, collapsing the weaker bonds in the
251 material. However, the biodegradability of these three concentrations of 3D scaffolds
252 after 28 days was approximately 30% - 60%, suggesting that the 3D scaffold material
253 may be used as long-term implant material.

254 Fig. 5 presents SEM image of the degradation of the 3D scaffold by various

255 enzymes. By comparison with the SEM image of the not-degraded PVA-g-starch 3D
256 scaffold in Fig. 1, the SEM image in the Fig. 5 indicates signs of degradation after six
257 days of enzyme treatment. Enzymatic degradation of the pores causes them to become
258 deformed or to be eliminated as presented in square frame (Fig. 5). This result
259 demonstrates that the 3D scaffold after cross-linking can be degraded by enzymes *in vivo*,
260 and can be utilized in tissue engineering applications.

261 **3.6. *In vitro* test**

262 To elucidate the cell culturing conditions in a 3D scaffold, mouse NIH3T3
263 fibroblasts were implanted into a 3D scaffold and the consequent cell growth. Fig. 6 plots
264 the growth curves of mouse NIH3T3 fibroblasts cells that were implanted in the 3D
265 scaffold. As the culture time increased, the number of cells also increased, reaching 10-15
266 $\times 10^4$ in 144 hours, indicating that the material supported cell proliferation. Fig. 7
267 presents the electron microscope SEM and EDS analysis diagrams of cells that were
268 implanted in the 3D scaffold compared with original 3D scaffold. The photograph
269 significant reveals cell growth; EDS analysis confirmed the presence of phosphorus and
270 calcium, proving that cells indeed grew on the cross-linked PVA-g-starch 3D scaffold.

271 **4. Conclusions**

272 The cross-linked PVA-g-starch 3D scaffold reveals that is highly porous and easily
273 formed using a homogenizer at 500 rpm. Formaldehyde (aldehyde group) can react with
274 PVA and starch (hydroxyl groups) under the presence of an acid catalyst, and forming
275 rings structure of 1, 3-dioxane. The FT-IR analysis demonstrates that the PVA-g-starch
276 had been successfully prepared. The produced 3D scaffolds have highly porosity; can
277 keep a large number of water. The absorption of water of 3D scaffold increased
278 significantly with starch concentration, absorbency of up to 800%. The wet state tensile
279 strengths of the 3D scaffolds all exceeded 3.6×10^{-2} MPa, and of these 3D scaffolds

280 exhibited excellent elongation at breakage and excellent elasticity. A PVA and starch all
281 have biodegradability. The high concentration of starch is presumed to make the structure
282 of scaffold denser and more complete, making it more difficult for the enzymes to
283 degrade. However, the biodegradability of PVA-g-starch 3D scaffolds after 28 days was
284 approximately 30% - 60%, suggesting that the 3D scaffold material may be used as
285 long-term implant material. *In vitro* test, the number of cells gradually increased with the
286 cultivation time in the 3D scaffold, comparison with original 3D scaffold. The EDS
287 analysis of the surface of the scaffold revealed the presence of phosphorus and calcium
288 and those normal cells can attach to, and grow on it. It is suggesting that the 3D scaffold
289 is biocompatible, allowing the proliferation, adhesion and growth of cells. The
290 PVA-g-starch 3D scaffolds have potential use for tissue engineering.

291

292 **References**

- 293 Asran, A.Sh. Henning, S., & Michler, G.H. (2010). Polyvinyl
294 alcohol–collagen–hydroxyapatite biocomposite nanofibrous scaffold: Mimicking the
295 key features of natural bone at the nanoscale level. *Polymer*, *51*(4), 868-876.
- 296 Castillejo, M., Rebollar, E., Oujja, M., Sanz, M., Selimis, A., Sigletou, M., Stelios,
297 Psycharakis, A.R., & Fotakis, C. (2012). Fabrication of porous biopolymer substrates
298 for cell growth by UV laser: The role of pulse duration. *Applied Surface Science*,
299 *258*(23), 8919-8927.
- 300 Chen, G., Ushida, T., & Tateshi, T. (2000). A biodegradable hybrid sponge nested with
301 collagen microsponges. *J. Biomed Mater Res.*, *51*(2), 273-279.
- 302 Duarte, A.R.C., Mano, J.F., & Reis, R.L. (2010). Enzymatic degradation of 3D scaffolds
303 of starch-poly-(ϵ -caprolactone) prepared by supercritical fluid technology. *Polymer*
304 *Degradation and Stability*, *95*(10), 2110-2117.
- 305 Ghosh, S.b., Gutierrez, V., Fernandez, C., Miguel A., Rodriguez-Perez, V. J. C., Reis R.L.,
306 & Mano, J.F., (2008). Dynamic mechanical behavior of starch-based scaffolds in dry

- 307 and physiologically simulated conditions: Effect of porosity and pore size. *Acta*
308 *Biomaterialia*, 4(4), 950-959.
- 309 Gomes, M.E., Godinho, J.S., Tchalamov, D., Cunha, A.M., & Reis, R.L. (2002).
310 Alternative tissue engineering scaffolds based on starch: processing methodologies,
311 morphology, degradation and mechanical properties. *Materials Science and*
312 *Engineering C*, 20(1-2), 19-26.
- 313 Hsieh, W.-C., Chen, Uang, W.-N., Yang, S.-J., & Chou, H.-H. (2011). 3D tissue culture
314 and fermentation of poly(3-hydroxybutyrate-co-3-hydroxyvalerate) from
315 *Burkholderia cepacia* D1. *Journal of the Taiwan Institute of Chemical Engineers*,
316 42(6), 883-888.
- 317 Jiang, J., Kojima, N., Kinoshita, T., Miyajima, A., Yan, W., & Sakai, Y. (2004).
318 Cultivation and induction of fetal liver cells in poly-L-lactic acid scaffold. *Materials*
319 *Science and Engineering C*, 24(3), 361-363.
- 320 Jiang, S., Liu, S., & Feng W.H. (2011). PVA hydrogel properties for biomedical
321 application. *Journal of the mechanical behavior of biomedical materials*, 4(7),
322 1228-1233.
- 323 Kuo, C.-F., Tsao, N., Chou, H.-H., Liu, Y.-L., & Hsieh, W.-C. (2012). Release of
324 FITC-BSA from poly(L-lactic acid) microspheres analysis using flow cytometry.
325 *Colloids & Surfaces B : Biointerfaces*, 89(1), 271-276.
- 326 Lahiji, A., Sohrabi, A., Hungerford, D.S., & Frondoza, C.G. (2000). Chitosan supports the
327 expression of extracellular matrix proteins in human osteoblasts and chondrocytes. *J.*
328 *Biomed Mater Res.*, 51(4), 586-595.
- 329 Lanza, R.P., Langer, R., & Vacanti, J. P. (1999). Principles of tissue engineering. (2nd)
- 330 Lee, C.T., Kung, P.H., & Lee, Y.D. (2005). Preparation of poly(vinyl alcohol)-chondroitin
331 sulfate hydrogel as matrices in tissue engineering. *Carbohydrate Polymer*, 61(3),
332 348-354.
- 333 Li, Z., Ramay, H.R., Hauch, K.D., Xiao, D., & Zhang, M. (2005). Chitosan–alginate

- 334 hybrid scaffolds for bone tissue engineering. *Biomaterials*, 26(18), 3919-3928.
- 335 Liao, H.h., Qi, R.l., Shen, M.w., Cao, X.Y., Guo, R., Zhang, Y.Z., & Shi, X.Y. (2011).
336 Improved cellular response on multiwalled carbon nanotube-incorporated
337 electrospun polyvinyl alcohol/chitosan nanofibrous scaffolds. *Colloids and Surfaces*
338 *B: Biointerfaces*, 84(2), 528-535.
- 339 Mansur, H.S., & Costa H.S. (2008). Nanostructured poly(vinyl alcohol)/bioactive glass
340 and poly(vinyl alcohol)/chitosan/bioactive glass hybrid scaffolds for biomedical
341 applications. *Chemical Engineering Journal*, 137(1), 72-83.
- 342 Mohan, N., & Nair, P.D. (2008). Polyvinyl Alcohol-Poly(caprolactone) Semi IPN
343 Scaffold With Implication for Cartilage Tissue Engineering. *Journal of Biomedical*
344 *Materials Research Part B: Applied Biomaterials*, 84B(2), 584-594.
- 345 Mohan, N., Nair, P.D., & Tabata, Y. (2010). Growth factor-mediated effects on
346 chondrogenic differentiation of mesenchymal stem cells in 3D semi-IPN poly(vinyl
347 alcohol)-poly(caprolactone) scaffolds. *Journal of Biomedical Materials Research*
348 *Part A*, 94A(1), 146-159.
- 349 Nie, L., Chen, D., Suo, J.P., Zou, P., Feng, S.b., Yang, Q., Yang, S.h., & Ye, S.A. (2012).
350 Physicochemical characterization and biocompatibility in vitro of biphasic calcium
351 phosphate/polyvinyl alcohol scaffolds prepared by freeze-drying method for bone
352 tissue engineering applications. *Colloids and Surfaces B: Biointerfaces*, 100(1),
353 169-176.
- 354 Oh, S.H., Kang, S.G., Kim, E.S., Cho, S.H., & Lee, J.H. (2003). Fabrication and
355 characterization of hydrophilic poly(lactic-co-glycolic acid)/poly(vinyl alcohol)
356 blend cell scaffolds by melt-molding particulate-leaching method. *Biomaterials*,
357 24(22), 4011-4021.
- 358 Pashkuleva, I., López-Pérez, P.M., Azevedo, H.S., & Reis, R.L. (2010). Highly porous
359 and interconnected starch-based scaffolds: Production, characterization and surface
360 modification. *Materials Science and Engineering C*, 30(7), 981-989.

- 361 Poursamar, S.A., Azami, M., & Mozafari, M. (2011). Controllable synthesis and
362 characterization of porous polyvinyl alcohol/hydroxyapatite nanocomposite
363 scaffolds via an in situ colloidal technique. *Colloids and Surfaces B: Biointerfaces*,
364 *84(2)*, 310-316.
- 365 Rodrigues, A.I., Gomes, M.E., Leonor, I.B., & Reis, R.L. (2012). Bioactive starch-based
366 scaffolds and human adipose stem cells are a good combination for bone tissue
367 engineering. *Acta Biomaterialia*, *8(10)*, 3765-3776.
- 368 Salgado, A.J., Gomes, M.E., Chou, A., Coutinho, O.P., Reis, R.L., & Hutmacher, D.W.
369 (2002). Preliminary study on the adhesion and proliferation of human osteoblasts on
370 starch-based scaffolds. *Materials Science and Engineering C*, *20(1)*, 27-33.
- 371 Santos, T.C., Marques, A.P., Horing, B., Martins, A.R., Tuzlakoglu, K., Castro, A.G.,
372 Griensven, M., & Reis, R.L. (2010). In vivo short-term and long-term host reaction to
373 starch-based scaffolds. *Acta Biomaterialia*, *6(10)*, 4314-4326.
- 374 Sundaram, Jaya., Durance, T.D., & Wang, R. (2008). Porous scaffold of gelatin–starch
375 with nanohydroxyapatite composite processed via novel microwave vacuum drying.
376 *Acta Biomaterialia*, *4(4)*, 932-942.
- 377 Thomas, L.V., Arun, U., Remya, S., & Nair, P.D. (2009). A biodegradable and
378 biocompatible PVA–citric acid polyester with potential applications as matrix for
379 vascular tissue engineering. *J. Mater. Sci: Mater Med.*, *20(1)*, S259-S269.
- 380 Wang, Y.W., Wu, Q., & Chen, G.Q. (2004). Attachment, proliferation and differentiation
381 of osteoblasts on random biopolyester poly(3-hydroxybutyrate-co-3-hydroxyl
382 hexanoate) scaffolds. *Biomaterials*, *25(4)*, 669-675.
- 383 Xiao, C.M., & Yang, M. (2006). Controlled preparation of physical cross-linked
384 starch-g-PVA hydrogel. *Carbohydrate Polymers*, *64(1)*, 37-40.
- 385 Yoshimoto, H., Shin, Y.M., Terai, H. & Vacanti, J. P. (2003). A biodegradable nanofiber
386 scaffold by electrospinning and its potential for bone tissue engineering.
387 *Biomaterials*, *24(12)*, 207

388

389

Table caption

390

391

392

393

394

395

396 Table 1. Mechanical properties of various cross-linked PVA-g-starch 3D
397 scaffold under wet state.

398

399

400

401

402

403

404

405

406

407

408

409

410

411

412

413

414

415

416

417

418

419

420

421

422

423

424 Table 1. Mechanical properties of various cross-linked PVA-g-starch 3D scaffold under

425 wet state.

Sample	Tensile strength (10^{-2} x MPa)	Elongation to break (%)	Young's modulus (10^{-2} x Gpa)	Porosity (%)
ST1	4.27	336	2.5	75
ST2	3.78	289	1.5	77
ST3	3.59	363	1.9	86

426

427 7-2082.

Figure captions

- Fig. 1. SEM image of various cross-linked PVA-g-starch 3D scaffolds. (Concentrations ratio of PVA and starch are ST1=1:0.5, ST2=1:0.75, and ST3=1:1)
- Fig. 2. FTIR spectrum of PVA, starch and cross-linked PVA-g-starch 3D scaffold.
- Fig. 3. Swelling ratio of various cross-linked PVA-g-starch 3D scaffolds. The above histogram is the actual forming figure of the cross-linked PVA-g-starch 3D scaffold. (Concentrations ratio of PVA and starch are ST1=1:0.5, ST2=1:0.75, and ST3=1:1)
- Fig. 4. Weight loss of various cross-linked PVA-g-starch 3D scaffolds in the various enzymatic degradation at 28 days. (■: lipase, ◆: α -amylase, ▲: lysozyme, ●: control)
- Fig. 5. SEM image of degraded PVA-g-starch 3D scaffolds by enzyme. (a : lipase, b : lysozyme)
- Fig. 6. Cell proliferation of NIH 3T3 cells on various cross-linked PVA-g-starch 3D scaffolds as a function of time. (▲:ST1, ◆:ST2, ■: ST3)
- Fig. 7. SEM images of NIH3T3 cells on cross-linked PVA-g-starch 3D scaffold after 3 days of culture. (A: Original material, B & C : materials with Cells, X370 & X2000)

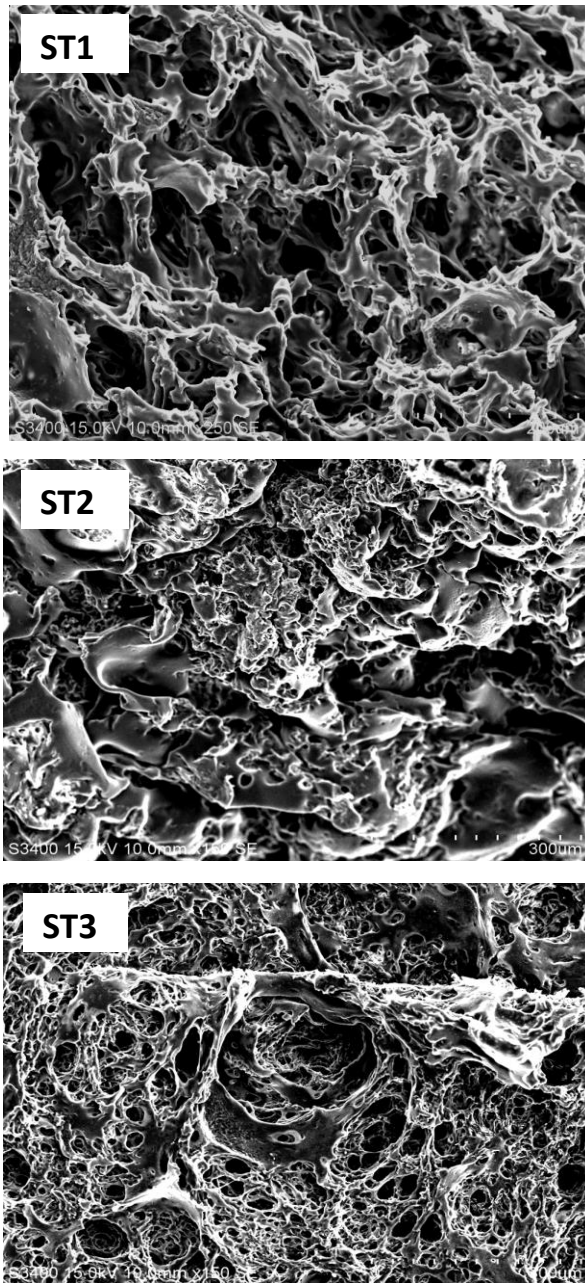


Fig. 1. SEM image of various cross-linked PVA-g-starch 3D scaffolds. (Concentrations ratio of PVA and starch are ST1=1:0.5, ST2=1:0.75, and ST3=1:1)

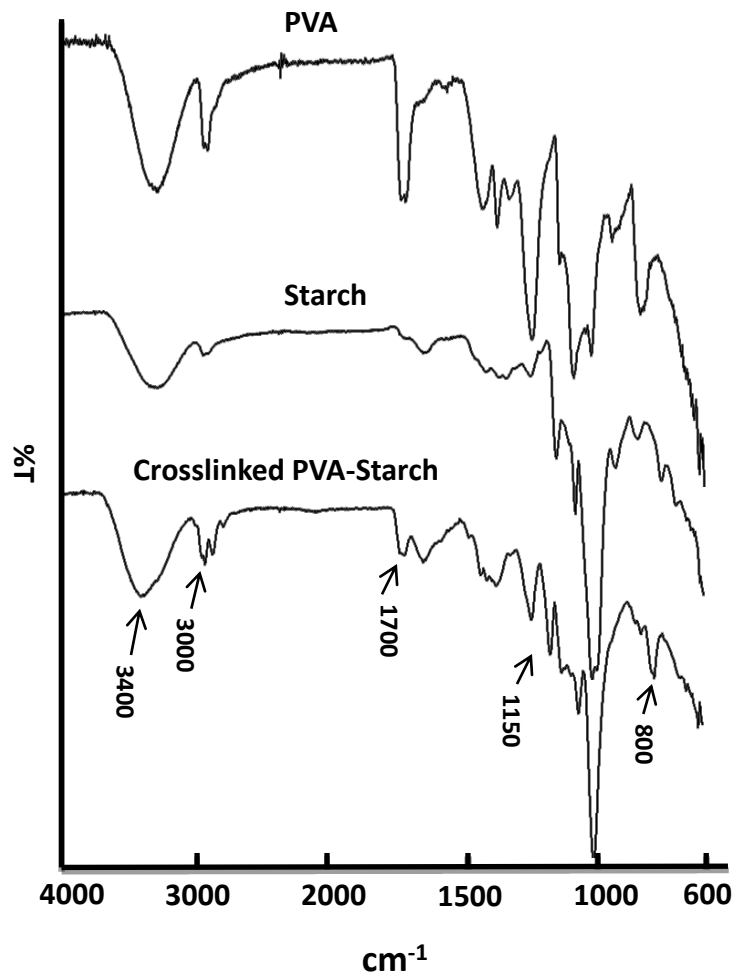


Fig. 2. FTIR spectrum of PVA, starch and cross-linked PVA-g-starch 3D scaffold.

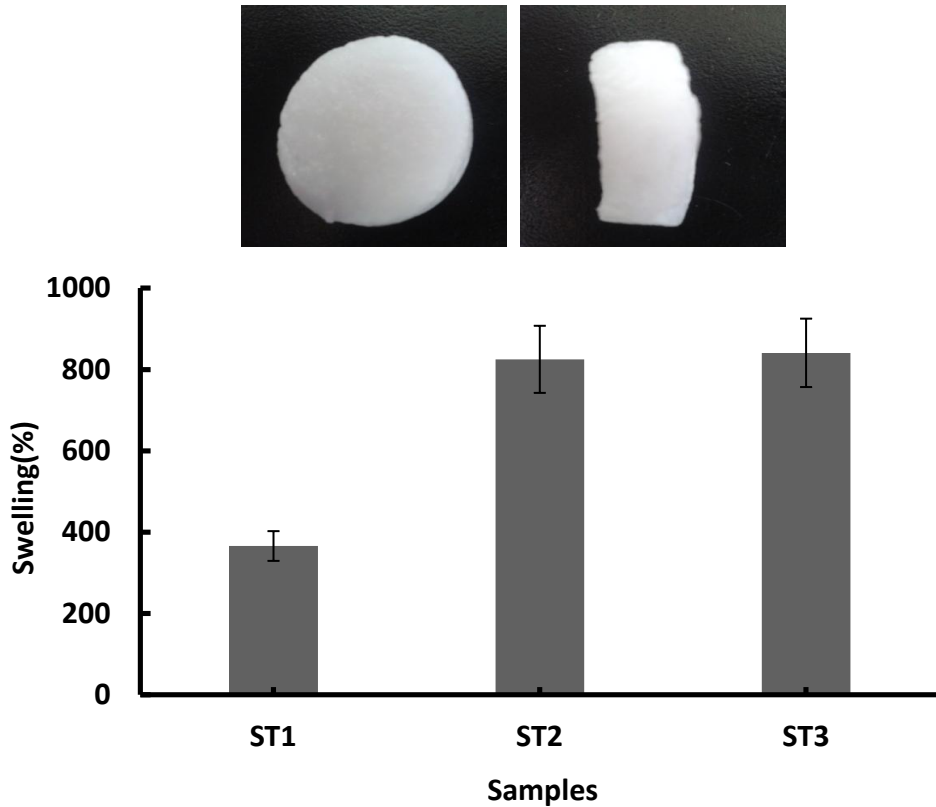


Fig. 3. Swelling ratio of various cross-linked PVA-g-starch 3D scaffolds. The above histogram is the actual forming figure of the cross-linked PVA-g-starch 3D scaffold. (Concentrations ratio of PVA and starch are ST1=1:0.5, ST2=1:0.75, and ST3=1:1)

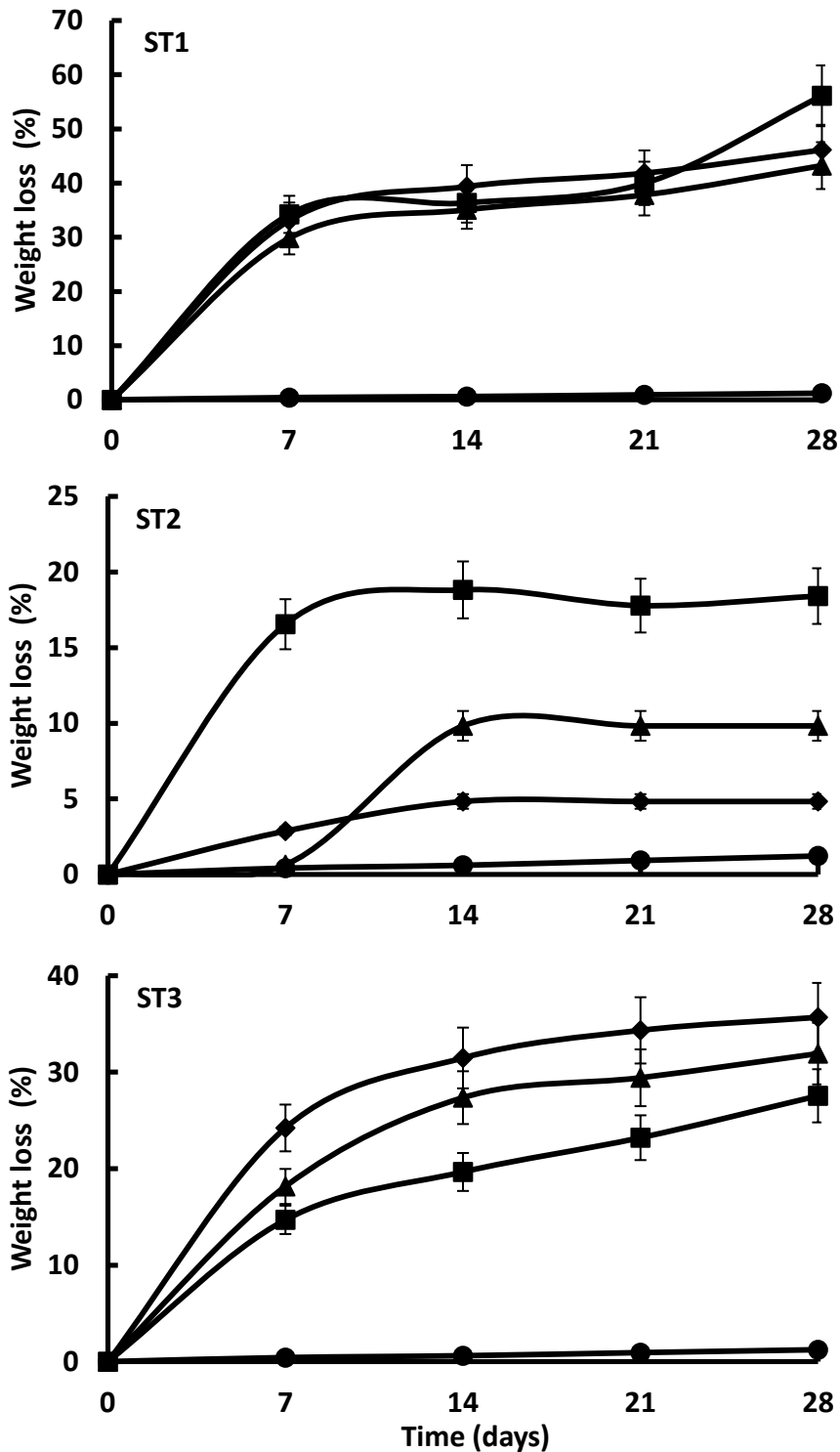


Fig. 4. Weight loss of various cross-linked PVA-g-starch 3D scaffolds in the various enzymatic degradation at 28 days. (■: lipase, ◆: α-amylase, ▲: lysozyme, ●: control)

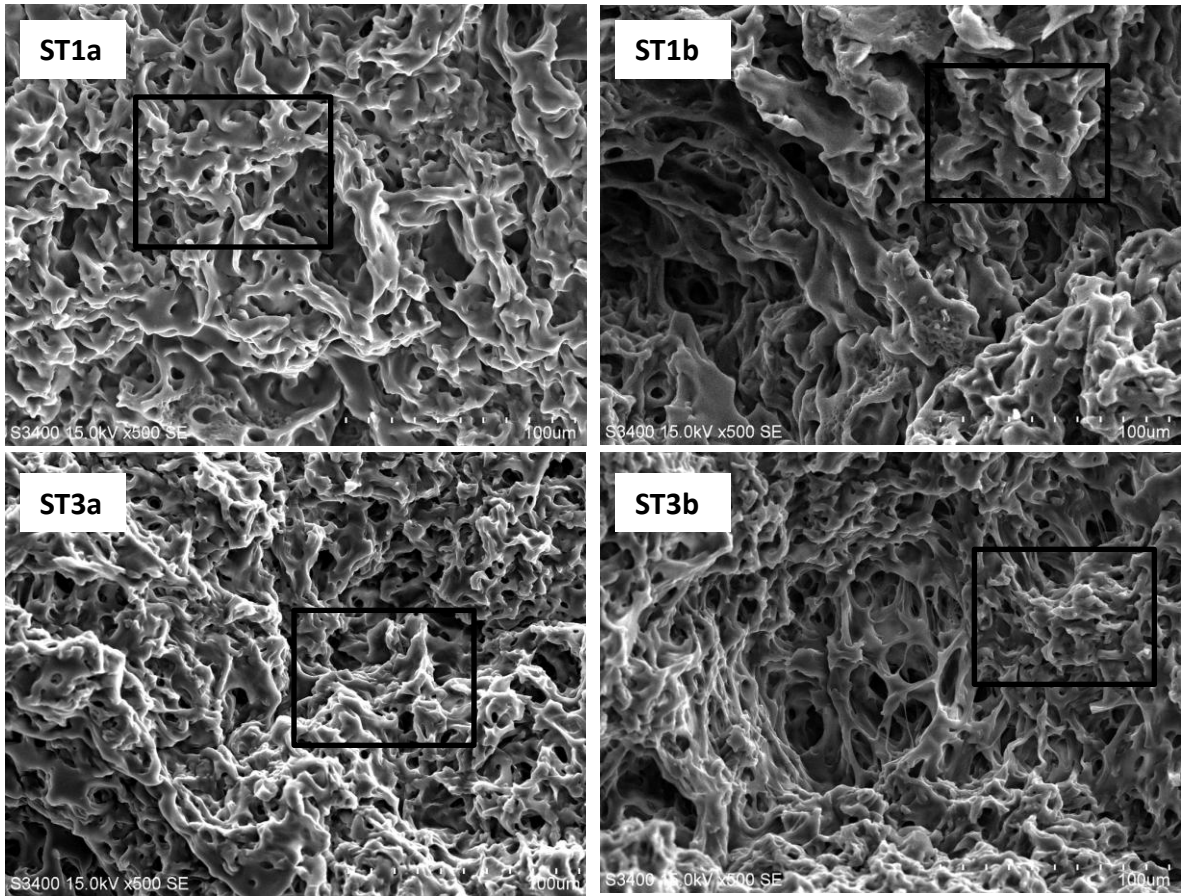


Fig. 5. SEM image of degraded PVA-g-starch 3D scaffolds by enzyme. (a : lipase, b : lysozyme)

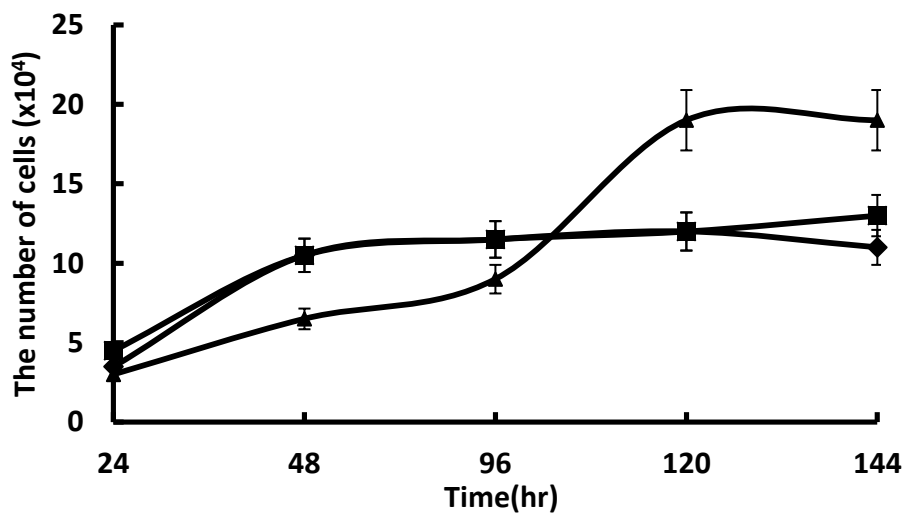


Fig. 6. Cell proliferation of NIH 3T3 cells on various cross-linked PVA-g-starch 3D scaffolds as a function of time. (▲:ST1、◆:ST2、■: ST3)

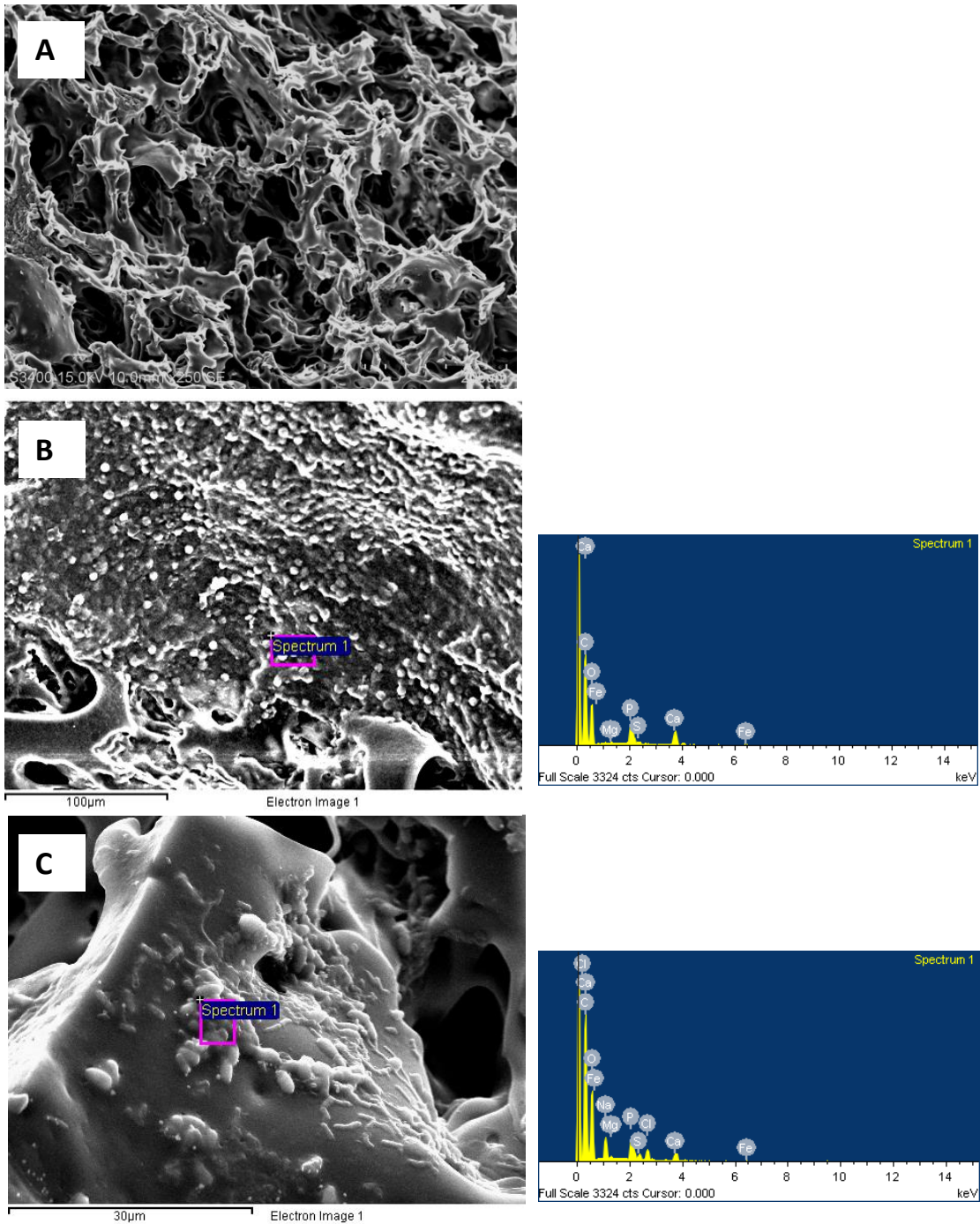


Fig. 7. SEM images of NIH3T3 cells on cross-linked PVA-g-starch 3D scaffold after 3 days of culture. (A: Original material, B & C : materials with Cells, X370 & X2000)